Applied Chemical Engineering (2021) Volume 4 Issue 2
doi:10.24294/ace.v4i2.1355

ORIGINAL RESEARCH ARTICLE

Density function theory on the electronic structure property of anatase TiO_2 doped by N or C with different percents

Zongbao Li[1*], Lichao Jia[2], Xia Wang[3], Liangjie Wang[1]

[1] *Department of Physics & Electronic Science, Tongren University, Guizhou 554300, China. E-mail: zongbaoli1982@163.com*

[2] *School of Materials Science and Engineering, State Key Lab of Material Processing and Die & Mould Technology, Huazhong University of Science and Technology, Wuhan 430074, China*

[3] *Department of Biology & Chemistry, Tongren University, Guizhou 554300, China*

ABSTRACT

Formation energy, crystal structure and electronic structure of C, N doped anatase TiO_2 are calculated based on the density functional theory of plane-wave ultrasoft pseudopotential. Results indicate that, due to doping of the C or N atoms in anatase TiO_2, the lattice distorts obviously. The substitution of C tends to Ti site while N tends to O site. All the substitutions lead to the red shift of the optical absorption and increasing coefficient of light absorption. When N concentrations are 2.08% and 3.13% in N-doped TiO_2, the highest photocatalytic activity is obtained, while it is 2.08% for C-doped one.

Keywords: Anatase TiO_2; DFT; N-doped; C-doped; Formation Energy

ARTICLE INFO

Received: 13 August 2021
Accepted: 26 September 2021
Available online: 4 October 2021

1. Introduction

TiO_2 has been widely used in the conversion and storage of sunlight, photocatalytic oxidation-reduction of greenhouse gases and degradation of environmental organic pollutants, and has become the most potential photocatalyst[1–4]. However, based on the large band gap (3–3.2 eV), pure TiO_2 is only sensitive to ultraviolet light ($\lambda < 400$ nm), but it does not respond to the visible light accounting for 43% of the solar energy. Therefore, how to improve TiO_2 and expand its light response range from ultraviolet light region to visible light region has become the focus of current research. At present, the modification methods of TiO_2 mainly include non-metallic ion doping[5], semiconductor recombination[6], metal deposition[7], etc. However, it is found that transition metal ion doping can improve the photocatalytic activity of TiO_2 by relying on the migration of d electrons, but transition metal doping will promote carrier recombination and reduce the thermal stability of TiO_2[8]. A large number of experiments have also proved that the surface deposition of noble metal atoms, such as Ag/TiO_2[9], Pt/TiO_2[10], Sn/TiO_2[11], etc., plays a significant role in improving the photocatalytic activity of TiO_2. However, the extensive use of precious metals will inevitably increase the manufacturing cost, which is not conducive to the promotion of industrial production. Since it was reported that N-doped

TiO_2 has better photocatalytic activity and proposed that non-metallic doping can effectively reduce the band gap and adjust the energy band distribution of TiO_2[12], reports of TiO_2 doped with non-metal such as C[13], N[14], S[15] and B have increased.

$TiO_{2\text{-}X}N_x$ visible light response catalyst was prepared by NO_x doping N[12], but it has the disadvantages of low preparation efficiency and high cost[12]. Cui *et al.* obtained N-doped TiO_2 by calcining TiN in air and found that it can effectively catalyze the decomposition of water to produce H_2 under visible light[16]. The N-doped TiO_2 prepared by Liu Shouxin et al. has good light response efficiency under visible light[17]. For C-doping, Khan *et al.* found that C-doped TiO_2 films have two absorption bands at 440 nm and 535 nm[18]; Sakthivel and Kisch *et al.* reported that the photocatalytic efficiency of C/TiO_2 prepared by them was 5 times higher than that of un-doped[19]. Chen *et al.* prepared C, N and S single doped anatase TiO_2 powder by the high temperature oxidation method[20]. It was found that the visible light photocatalytic effect of N doping was the most obvious, while the impurity energy level of C was deeper. Because the substitution mode of doped particles in the material preparation process is greatly affected by the growth environment, the results of C and N doped TiO_2 systems will be quite different in different chemical environments. However, so far, the effects of doping methods, defect forms and doping ratio on photocatalytic properties have not been systematically reported.

Based on the density functional theory, the formation energy, crystal structure and electronic structure of C and N doped TiO_2 were calculated by using the super cell model. The position of substitution doping of C and N atoms and the effects of different doping ratios on the electronic structure and optical properties of TiO_2 are analyzed theoretically, and the effects of single doping on the properties of TiO_2 are revealed.

2. Calculation methods

The plane-wave ultrasoft pseudopotential method based on the density functional theory, we adopt the GGA + PBE exchange correlation method for TiO_2 2 × 2 × 2 to obtain the best structural parameters[21]. Select the plane wave truncation energy in the inverted lattice space: $E_{\text{cut}} = 400$ eV, and point K is 4 × 4 × 4. The accuracy of self-consistent field operation is set as that the single atom energy converges to 2.0×10^{-6} eV[22]. Because the traditional GGA theory underestimates the energy band in energy band calculation, in order to form a comparison with the experiment, the calculated energy band structure and density of states are modified by the GGA + U method[23] to make it consistent with the experimental results. The correction parameters selected in the calculation are: $U = 6.3$ eV and $J = 1$ eV[24]. All doping parameters selected later adopt the same settings to ensure the comparability of calculation results. To construct multi concentration doping in anatase TiO_2 2 × 2 × 2 based on the optimized super cell structure, and randomly replace 1–4 O or Ti atoms in the lattice with N or C, the doping ratio is similar to the experimental scheme. Because of the extremely high formation energy and instability, the interstitial defect models of N and C are not discussed in this paper. In addition, due to the proximity of N and O atoms in the periodic table, it has been proved that N can only replace O atoms; however, for C substitution, due to the particularity of its position in the periodic table, its doping mode has not been clear. In order to obtain its real substitution mode, this paper adopts different methods to replace Ti and O sites respectively, and optimizes the structure on this basis. All calculations in this paper are carried out in VASP software package[25,26].

3. Results and discussion

In order to effectively discuss the effect of different proportion of C and N doping on TiO_2, the formation energy after doping at different positions of C and N was calculated. According to the special position of C in the periodic table, it is considered that C^{2-} and C^{4+} ions may appear in TiO_2 crystals. Based on the stability conditions of different doped systems, in order to further clarify the real occupied position of elements in TiO_2 after doping, the formation energy E_{form} of impurities in different doped systems is calculated:

$$E_{\text{form}} = E_{\text{doped}} - E_{\text{pure}} - m \bullet \mu_{\text{C}} - n \bullet \mu_{\text{N}} + u \bullet \mu_{\text{O}} + v \bullet \mu_{\text{Ti}} \quad (1)$$

In the formula, E_{pure} and E_{doped} are the energies of pre-doping and post-doping anatase TiO_2 respectively. μ_{N}, μ_{C}, μ_{O} and μ_{Ti} represent the chemical potentials of N, C, O and Ti respectively; m, n, u, v are the numbers of doped atoms and the number of substituted atoms in the corresponding system. The above formula is used to calculate the formation of C and N replacing one Ti or O respectively, as shown in **Table 1**.

Table1. Formation energies E_{form} of different doped TiO_2

	N@O	N@Ti	C@O	C@Ti
E_{form} /eV	4.37	7.51	6.51	5.27

As can be seen from **Table 1**, the formation energy of N@O is lower than that of N@Ti, and the formation energy of C@Ti is lower than that of C@O. It is indicated that the primary N is inclined to O and C is inclined to Ti. This result is different from the experimental conjecture of Zhang Xiaoyan *et al.*[27].

Table 2. Lattice parameters and average bond lengths of the doped TiO_2 after geometry optimization (in Å)

	a	b	c	Ti-O	Ti-N	C-O
Pure	7.577	7.577	9.541	1.976		
N@O	7.603	7.570	9.508	1.980	2.008	
C@Ti	7.786	7.786	9.389	1.961		1.242

Table 2 lists the structural parameters of the three systems after structural optimization. As can be seen from **Table 2**, the optimized 2 × 2 × 1 the lattice parameters of pure TiO_2 super cells are a = b = 7.577 Å and C = 9.541 Å, which are consistent with the experimental results[4]. After doping, due to the different ion radii of impurity elements, the symmetry of crystal structure decreases and the lattice is distorted. Because the radius of N^{3-} ion is larger than that of O^{2-} ion, the Ti-N bond length after N doping is longer than that of un-doped Ti–O bond. The radius of C^{4+} ion is 0.16 Å, which is much smaller than 0.68 Å of Ti^{4+} ion. Therefore, the C–O bond formed by C replacing Ti is much smaller than that of Ti–O bond (1.961 Å), only 1.242 Å. Due to the doping of impurity ions, the lattice distortion will also lead to the generation of internal dipole moment. The change of dipole moment can promote the photocatalytic performance of TiO_2.

3.1 Electronic structure of N-doped TiO_2 with different concentrations

Based on the displacement results, the variation trend of doping amount and material properties of N@O system was studied. Based on this model, the energy band structure and density of states of TiO_2 under various proportions are calculated, as shown in **Figures 1** and **2**. After N atoms in the lattice replace some O atoms, O–Ti–N bonds are formed in the lattice, and the crystal structure is distorted due to the difference between the radii of N and O atoms, resulting in the change of the doped band gap (*E*g) and the bandwidth between the impurity energy level and the bottom of the conduction band (Im-CBM), see **Table 3** for specific values. It can be seen from **Figure 1** and **Table 2** that N doping has little effect on the band gap width, and new impurity levels are generated at the top of the valence band of the four doped structures. When the impurity energy level is ignored, the band gap width is minimum at 2.08% (2.97 eV). If the auxiliary effect of impurity energy levels on the transition is considered, the superposition of impurity energy levels will move the absorption band edge of TiO_2 to the visible region. With the increase of doping concentration, the density of impurity energy level increases, which increases the transition probability of electrons. By comparing the density of impurity energy levels near the Fermi plane in **Figures 1** and **2**, it can be seen from **Figure 2** that when the doping ratio is 3.13%, the probability of ion transition is the largest, which is the better doping ratio. When the doping concentration continues to increase (>4.17%), the impurity energy levels will overlap at the top of the valence band and move up the top of the whole valence band. This result is conducive to the transmission of photogenerated carriers under certain conditions, but if the N content is too high, it is easy to form TiN structure and make the doped system cash attribute and opaque in the visible region. With the increase of N content, it will also lead to a large number of defects in the lattice and become the composite center of electron hole pairs, so as to reduce the photocatalytic activity of the material. Therefore, N doping can improve the photocatalytic performance of TiO_2 only in the appropriate concentration range.

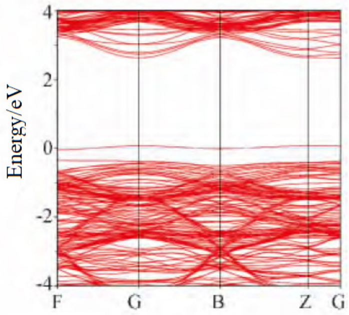

(a) 1.04%

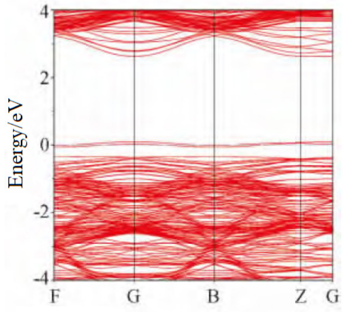

(b) 2.08%

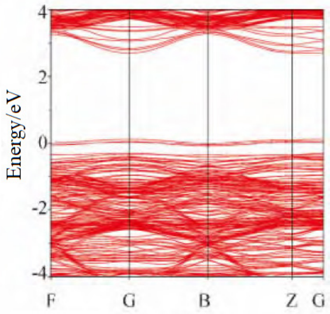

(c) 3.13%

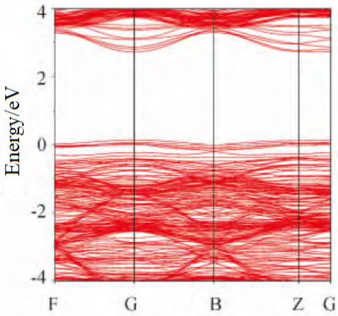

(d) 4.17%

Figure 1. Band structure for N-doped configurations with various doping levels.

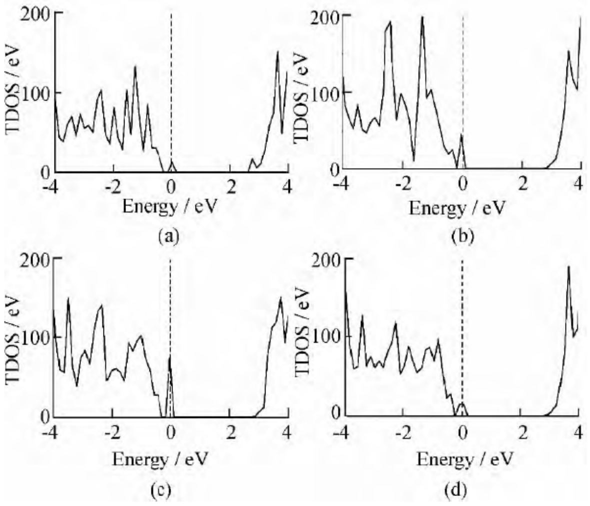

Figure 2. Total DOS of N-doped configurations with different ratios.

Table 3. Band gaps of N-doped configurations with different ratio (in eV)

Ratio	1.04%	2.08%	3.13%	4.17%
Eg	2.99	2.97	3.00	2.98
Im-CBM	2.56	2.53	2.58	2.60

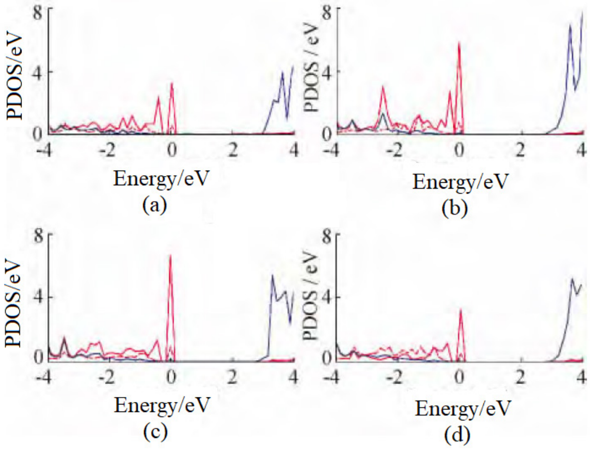

Figure 3. PDOS for N-doped configurations. N-2p and O-2p are shown with red solid and dash lines while blue ones indicate the Ti-3d levels.

In order to further understand the effect of N doping on TiO_2 energy level, the partial density of states of different doping concentrations are given, as shown in **Figure 3**. The impurity level near the Fermi level is mainly composed of N-2p state and relaxes at the top of the valence band, while the contribution of O-2p and Ti-3d States is small. It can be seen from the above comparison that after N doping, the position of the valence band top of the system is mainly determined by the N-2p state, and the O-2p state overlaps with N-2p, increasing the energy band density. The conduction band bottom of doped and un-doped TiO_2 is determined by Ti-3d state without obvious change. Given that the doping concentration is 2.08% and 3.13%, the Ti-3d state in the conduction band moves down slightly due to the p-d hybridization between N-2p and Ti-3d states.

It can be seen from the above analysis that when the doping concentration is low, the change of doping concentration has no obvious effect on the electronic structure of TiO_2, and the best content of N is 2.08% and 3.13%, which is the most favorable to improve the photocatalytic performance of TiO_2.

3.2 Electronic structure of C-doped TiO_2 with different concentrations

Based on the fact that C atoms in the single doped system tend to replace Ti atoms and exist in the form of C^{4+} cations, when constructing the C-doped TiO_2 crystal model, all calculations only consider the substitution of C atoms for Ti atoms and ignore the substitution of O atoms. **Figure 4** shows the band structure of C-doped TiO_2 with different concentrations. As can be seen from **Figure 4**, due to the nonmetallic nature of C, although it replaces Ti, the impurity level is not introduced into the band gap, but directly causes the conduction band to move to the low energy level, reduces the band gap width and increases the transition probability of electrons. Comparing the band gap widths of different doping concentrations, it can be seen that when the doping amount is 3.13% and 4.17%, the band gap width is the same, both of which are 2.51 eV; when the doping concentration is 1.04%, the band gap is the largest, which is 2.60 eV; when the doping concentration is 2.08%, the band gap is the smallest, which is 2.30 eV. It is proved that TiO_2 has obvious red shift after doping, especially when the C doping concentration is 2.08%.

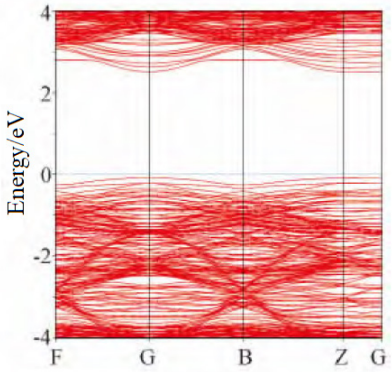

(a) 1.04%

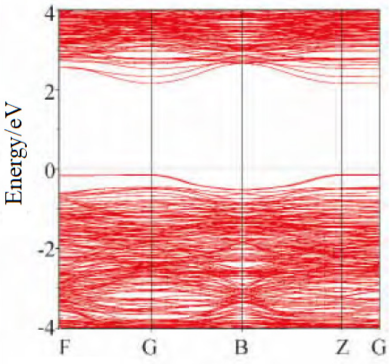

(b) 2.08%

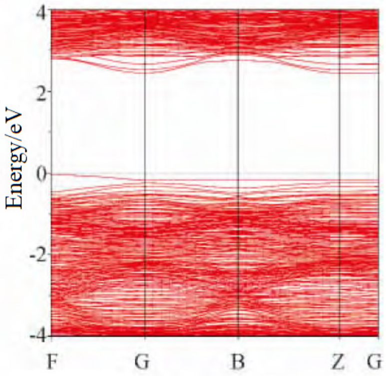

(c) 3.13%

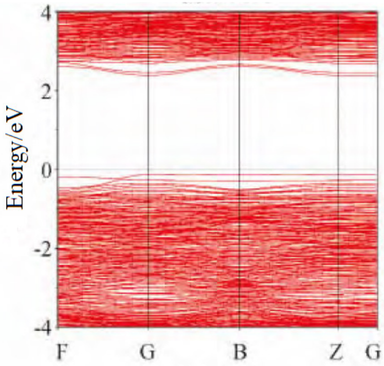

(d) 4.17%

Figure 4. Band structure for C-doped configurations with various doping levels.

In order to further reveal the concentration effect of C on TiO_2 doping, the partial density of states of doped systems with different concentrations are also calculated, as shown in **Figure 5**. It can be seen from **Figure 5** that the valence band of C-doped TiO_2 is mainly composed of O-2p state and T-3d state, and mainly occupies the low energy region. The O-2p state mainly contributes to the energy level near the Fermi plane and determines the position of the top of the valence band; the conduction band is mainly composed of Ti-3d state and C-2p state, and the strong pd orbital hybridization makes the conduction band move down obviously, so as to reduce the band gap. When the doping concentration is 2.08% and 4.17%, the pd hybrid phenomenon between Ti-3d state and C-2p state is very obvious, and a strong hybrid peak appears. By comparing the density of states of O-2p state in different systems, it can be seen that when the doping concentration is 4.17%, the impurity peak of O-2p state near Fermi level is significantly stronger than that of the other three doping cases, which proves that the probability of valence electron guide band transition increases under visible light, which is conducive to the improvement of photocatalytic efficiency of TiO_2.

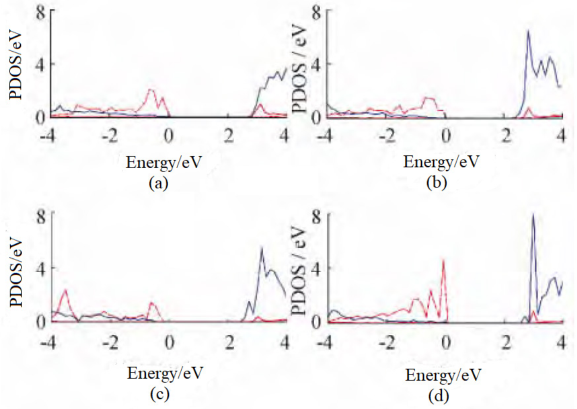

(a) (b) (c) (d)

Figure 5. PDOS for C-doped configurations with different ratios.

It can be seen from the above analysis that when C changes with doping concentration, the hybridization effect between C-2p state and Ti-3d state directly leads to the movement of the conduction band to the low energy direction, which leads to the reduction of the band gap and the obvious red shift of the absorption band edge. According to the comparison of band gap width, it can be seen that when the doping concentration is 2.08%, the response to visible light is the strongest, and the catalytic activity should be the highest. Compared with the results of N-doped TiO_2, it can be seen that the concentration effect has a more obvious effect on the photocatalytic performance of the C-doped system.

4. Conclusion

Based on the density functional theory, the formation energy, lattice structure and electronic structure of anatase TiO_2 doped with different proportions of N and C atoms were calculated. By comparing the formation energies, it can be seen that N atoms tend to replace O sites and C replace Ti sites; through the analysis of energy band and band density of doped crystals with different proportions, it can be seen that when N is doped at low concentration, the effect of doping concentration on the electronic structure of TiO_2 is not obvious, and when N content is 2.08% and 3.13%, TiO_2 has the best response to visible light, which has better photocatalytic performance; when the C doping concentration is 2.08%, its response to visible light is the best. Compared with N-doped TiO_2, the concentration effect has a more obvious effect on the photocatalytic performance of C-substituted Ti-doped system.

Conflict of interest

The authors declare that they have no conflict of interest.

Acknowledgements

This research was supported by the Guizhou Natural Science Foundation ([2012]17), the key program of Guizhou Provincial Department of Education ([2013]182), and the Scientific Research Fund of Tongren University (S1232).

References

1. Fujishima A, Honda K. Electrochemical photolysis of water at a semiconductor electrode. Nature 1972; 238: 37–39.
2. Gole JL, Stout JD, C Burda C, *et al.* Highly efficient formation of visible light tunable $TiO_{2-x}N_x$ photo-

catalysts and their transformation at the nanoscale. The Journal of Physical Chemistry B 2004; 108(4): 1230–1240.

3. Linsebigler AL, Lu G, Yates JT Jr. Photocatalysis on TiO_2 surfaces: Principles, mechanisms, and selected results. Chemical Reviews 1995; 95(3): 735–758.
4. Fujishima A, Rao TN, Tryk DA. Titanium dioxide photocatalysis. Journal of Photochemistry and Photobiology C: Photochemistry Reviews 2000; 1(1): 1–21.
5. Asahit R, Morikawa T, Ohwaki T, *et al.* Visible-light photocatalysis in nitrogen-doped titanium oxides. Science 2001; 293(5528): 269–271.
6. Cheng G, Zhou X, Li Y, *et al.* La^{3+} modification of ZnO-TiO_2 coupled semiconductors and their photocatalytic activity. Chinese Journal of Catalysis 2007; 28(10): 885–889.
7. Li Z, Wang X, Jia L. Synergistic effects in Fe/N co-doped anatase TiO_2 (101) surface: A theoretical study based on density functional theory calculation. Acta Physica Sinica 2013; (20): 1–5.
8. Hou Q, Zhang Z, Li C. First-principles study of the electronic life and red shift effect of Sm-doped anatase TiO_2. Journal of Functional Materials 2012; 43(19): 2599–2604.
9. Subrahmanyam A, Biju KP, Rajesh P, *et al.* Surface modification of sol gel TiO_2 surface with sputtered metallic silver for Sun light photocatalytic activity: Initial studies. Solar Energy Materials and Solar Cells 2012; 101: 241–248.
10. Li Z, Wang X. First-principle study of electronic structure and enhanced visible-light photocatalytic activity of anatase TiO_2 through C and F codoping. Advanced Materials Research 2013; 746: 400–405.
11. Zhang MY, He GZ, Ding CC, *et al.* Mechanism of arsenate (V) adsorption on TiO_2 surfaces. Acta Physico-Chimica Sinica 2009; 25: 2034–2038.
12. Zheng S, Wu G, Liu L. First-principles calculations of P-doped anatase TiO_2. Acta Physica Sinica 2013; (4): 94–100.
13. Carp O, Huisman CL, Reller A. Photoinduced reactivity of titanium dioxide. Progress in Solid State Chemistry 2004; 32(1-2): 33–177.
14. Suda Y, Kawasaki H, Ueda T, *et al.* Preparation of high quality nitrogen doped TiO_2 thin film as a photocatalyst using a pulsed laser deposition method. Thin Solid Films 204; 453: 162–166.
15. Umebayashi T, Yamaki T, Itoh H. Band gap narrowing of titanium dioxide by sulfur doping. Applied Physics Letters 2002; 81: 454–456.
16. Cui X, Ma M, Zhang W. Nitrogen-doped TiO_2 from TiN and its visible light photoelectrochemical properties. Electrochemistry Communications 2008; 10 (3): 367–371.
17. Liu S, Chen X, Li X. Effect of N-doping on structure characteristics and photocatalytic activity of TiO_2 photocatalyst. Chinese Journal of Inorganic Chemistry 2008; 24(2): 253–259.
18. Khan SUM, Al-Shahry M, Ingler WB Jr. Efficient photochemical water splitting by a chemically modified n-TiO_2. Science 2002; 297(5590): 2243–2245.
19. Sakthivel S, Kisch H. Daylight photocatalysis by carbon-modified titanium dioxide. Angewandte Chemie International Edition 2003; 42(40): 4908–4911.
20. Chen X, Burda C. The electronic origin of the visible-light absorption properties of C-, N- and S-doped TiO_2 nanomaterials. Journal of the American Chemical Society 2008; 130(15): 5018–5019.
21. Monkhorst HJ, Pack JD. Special points for Brillouin-zone integrations. Physical Review B 1976; 13: 5188–5192.
22. Dudarev SL, Botton GA, Savrasov SY, *et al.* Electron-energy-loss spectra and the structural stability of nickel oxide: An LSDA + U study. Physical Review B 1998; 57: 1505–1509.
23. Kavan L, Grätzel M, Gilbert SE, *et al.* Electrochemical and photoelectrochemical investigation of single-crystal anatase. Journal of the American Chemical Society 1996; 118(28): 6716–6723.
24. Jia L, Wu C, Li Y, *et al.* Enhanced visible-light photocatalytic activity of anatase TiO_2 through N and S codoping. Applied Physics Letters 2011; 98(21): 211903–211905.
25. Kressea G, Furthmüller J. Efficiency of ab-initio total energy calculations for metals and semiconductors using a plane-wave basis set. Physical Review B 1996; 54(16): 11169–11186.
26. Perdew JP, Burke K, Ernzerhof M. Generalized gradient approximation made simple. Physical Review Letters 1996; 77: 3865–3868.
27. Zhang X, Cui X. Preparation and photocatalytic

hydrogen evolution performance of C-N Co-doped Nano TiO_2 photocatalysts. Acta Physico-Chimica Sinica 2009; 25(9): 1829–1834.